

## Seismic Performance Assessment of Existing Steel Buildings: A Case Study

Luigi Di Sarno<sup>1,a\*</sup>, Fabrizio Paolacci<sup>2,b</sup> and Anastasios G. Sextos<sup>3,c</sup>

<sup>1</sup>Department of Engineering, University of Sannio, Piazza Roma 21, Benevento, Italy

<sup>2</sup>Department of Engineering, Roma Tre University, Via Vito Volterra 62, Roma, Italy

<sup>3</sup>Department of Civil Engineering, University of Bristol, Queen's Building, University Walk, BS8 1TR, Bristol, UK & Aristotle University of Thessaloniki, Greece

<sup>a</sup>ldisarno@unisannio.it; <sup>b</sup>fabrizio.paolacci@uniroma3.it; <sup>c</sup>a.sextos@bristol.ac.uk

\*corresponding author

**Keywords:** Buildings, Frames, Seismic assessment, Performance criteria, Earthquakes.

**Abstract.** Numerous existing steel framed buildings located in earthquake prone regions world-wide were designed without seismic provisions. Slender beam-columns, as well as non-ductile beam-to-column connections have been employed for multi-storey moment-resisting frames (MRFs) built before the 80's. Thus, widespread damage due to brittle failure has been commonly observed in the past earthquakes for steel MRFs. A recent post-earthquake survey carried out in the aftermath of the 2016-2017 Central Italy seismic swarm has pointed out that steel structures may survive the shaking caused by several main-shocks and strong aftershocks without collapsing. Inevitably, significant lateral deformations are experienced, and, in turn, non-structural components are severely damaged thus inhibiting the use of the steel building structures. The present paper illustrates the outcomes of a recent preliminary numerical study carried out for the case of a steel MRF building located in Amatrice, Central Italy, which experienced a series of ground motion excitations suffering significant damage to the masonry infills without collapsing. A refined numerical model of the sample structure has been developed on the basis of the data collected on site. Given the lack of design drawings, the structure has been partially re-designed in compliance with the Italian regulations imposed at the time of construction employing the allowable stress method. The earthquake performance of the case study MRF has been then investigated through advanced nonlinear dynamic analyses and its structural performance has been evaluated according to Eurocode 8-Part 3 for existing buildings. The reliability of the codified approaches has been evaluated and possible improvements emphasized.

### Introduction

The recent 2016-2017 Central Italy earthquakes have emphasized that the widespread damage and structural collapses occur for low-to-medium rise steel buildings that do not incorporate ductile seismic detailing. The damage has been observed primarily in existing steel multi-storey residential buildings which exhibited low energy absorption and inadequate dissipation capacity. The insufficient horizontal stiffness of the frame and the masonry infills led to significant lateral drifts and buckling in the steel components, especially in the columns. Local damage (buckling) has been observed at the connections, because of the strut-action induced by the presence of the masonry infills and plaster for achieving adequate insulation for the residential buildings. Furthermore, several issues related to the accurate seismic performance assessment of existing steel moment resisting frames (MRFs) are still open due to the complex behaviour and the interaction between beam-to-column connections [1], as well as the presence of composite steel and concrete slabs and masonry infills (e.g. [2, 3, 4, 5] among many others). An additional reason is the lack of existing code-based rules (see, for example, Eurocode 8, Part 3 [6] in Europe and ASCE-SEI 41-13 [7], in the US) with specific recommendation as per efficient numerical modelling and safety checks for steel frames with infills.

Existing steel structures therefore, especially existing non-ductile MRFs, have been found particularly vulnerable to seismic loading in the previous earthquakes (e.g. [7]). Despite the extensive analytical and experimental research on new steel frames during the last decade [8, 9, 10, 11], actual post-quake data of observed data are limited while the advances in the structural assessment of existing steel MRFs buildings are equally scant, especially in Europe. In this context, the objective of this paper is to present the case of a steel structure in Central Italy that was subjected to a sequence of earthquakes exhibiting significant infill damage but relatively limited damage in its lateral load resisting system as a means to discuss code limitations and challenges in the design of MRFs.

## 2. OVERVIEW OF THE 2016 CENTRAL ITALY EARTHQUAKES

On the 24th of August 2016, a seismic sequence of events was initiated in Central Italy. The first main shock was of moment magnitude  $M_w$  6.0 and occurred at a depth of 4km. The epicenter of the August's shock was located in the North-East area of the province of Rieti, ca. 2.5km North West of the village of Accumoli. This is a zone of high seismic hazard that has seen damaging earthquakes in the recent past. The earthquake was initiated from a slip on the mount Vettore-mount Bove fault system [12], the maximum amplitude of which was approximately 1m, acting at a dip angle of 50 degrees to the horizontal. A series of aftershocks followed the above event until the  $M_w$ 5.9 Ussita earthquake that occurred on the 26<sup>th</sup> of October and the main-shock of October 30<sup>th</sup> ( $M_w$  6.5 and depth of 9km). The latter was the strongest event since 1980. The particular event had an epicenter 5km from Norcia, overlaying the northern part of the fault activated by the earthquake of August 24<sup>th</sup>. The seismic sequence occurred in a "seismic gap" created by past events as highlighted by the limited release of energy in that area in the past years [13].

Amatrice was one of the towns that was devastated during the earthquake with the majority of the residential buildings in its historic center collapsing. The accelerometric station of the town of Amatrice, is located along the highway leading to the town center, at the junction with the communal road to the Laga Mountains and is part of the Italian Strong Motion Network managed by the Department of Civil Protection. It recorded the entire seismic sequence between August and November, 2016. The five strongest recordings in terms of peak ground acceleration (PGA) together with the relevant magnitude and other intensity proxies (peak ground velocities and displacements, quoted as PGV, PGD, respectively) are summarized in Table 1.

Table 1. Stronger ground motions recorded at the accelerometric station of Amatrice during the August and November 2016 mainshocks (M/S) and aftershocks (A/S).

| Event | Date                                | $M_w$ | $M_L$ | $R_{epi}$ [km] | PGA [g] | PGV [cm/s] | PGD [cm] |
|-------|-------------------------------------|-------|-------|----------------|---------|------------|----------|
| M/S1  | 24 <sup>th</sup> Aug. 2016 01:36:32 | 6.0   | 6.0   | 8.494          | 0.850   | 43.549     | 8.544    |
| A/S1  | 24 <sup>th</sup> Aug. 2016 01:56:03 | 4.3   | 4.5   | 3.609          | 0.190   | 6.823      | 0.515    |
| A/S2  | 25 <sup>th</sup> Aug. 2016 12:36:06 | 4.4   | 4.3   | 3.587          | 0.228   | 9.555      | 0.587    |
| A/S3  | 26 <sup>th</sup> Aug. 2016 04:28:25 | 4.8   | 4.7   | 3.104          | 0.329   | 11.001     | 0.636    |
| M/S2  | 30 <sup>th</sup> Oct. 2016 06:40:18 | 6.5   | 6.1   | 26.436         | 0.521   | 37.915     | 7.457    |

It is noted that the  $M_w$ 5.9 Ussita earthquake of October 26<sup>th</sup> (19.18 UTC) is not included in this list since its PGA was only 0.09g at the site of interest. Even though the second main-shock (M/S2) of October 30<sup>th</sup> was of a higher magnitude, the recorded PGA (equal to 0.52g) was smaller compared to the first main-shock of August 24<sup>th</sup> (0.82g) as the epicentral distance was larger in the second case. The accelerometers are founded on soil that is classified as B according to the recent Italian Seismic Code [14]. However, given the location of the building studied next to the slope and the topography of the town of Amatrice, it is deemed probable that the actual intensity that the building experienced was higher.

## 3. DESCRIPTION OF THE CASE STUDY BUILDING

The sample steel framed structure is a multi-storey building with a basement and two-floors above ground and a loft. The structure is located in the via dei Bastioni, close to the main road Corso Umberto, in the

centre of municipality of Amatrice. The building plan layout is trapezoidal; it is 22.5m long and 6.6-8.5m wide. The interstorey height of the first and second floor is 3m; the total height is about 9m. The flooring systems consist of concrete slabs on a steel corrugated 10mm thick sheet; shear studs are not present, hence the composite action between steel and concrete is not ensured. The steel grade for all structural components of the framed structure is equivalent to S235, i.e. it corresponds to Fe360 ( $f_y=235\text{MPa}$ ). The columns of the frame are profiles with HEA 200 cross sections, while the beams are HEA 300 (interior beams) and HEA 160 (exterior beams). The beam-to-column connections are fully welded (moment-resisting frame). The infills consist of a double layer of perforated brick of the size of 12x25x8 mm. The roof is supported by steel trusses, while the truss elements are made of 2L60x6mm profiles.

For assessment purposes and given the lack of existing design drawings and the difficulty to access the higher floors due to safety reasons, the existing steel structure has been re-designed according to the provisions included in [15] to resist earthquake-induced loads, that were employed at the time of construction, i.e. before year 2000. It is assumed that the self-weight of the slab is  $4.88\text{ kN/m}^2$ . The live loads are assumed equal to  $2.00\text{ kN/m}^2$  for the intermediate storeys. The snow and wind loads are taken equal to  $3.76\text{ kN/m}^2$  and  $0.96\text{ kN/m}^2$ , respectively. Once the structural elements have been designed, they were also compared with the actual components of the buildings and were found in good agreement.

#### **4. STRUCTURAL MODELLING**

The structural system has been modeled with a refined three-dimensional finite element model. Rigid offsets were implemented to account for the rigidity of the beam-to-column connections. Such offsets were taken equal to 15cm and 10cm at each end of the columns and beams, respectively. Diaphragmatic action was assumed at the first and second floors to account for the presence of the concrete slab on the steel corrugated sheet. It is noted that the roof does not have any rigid diaphragm. Appropriate checks, utilizing an equivalent-beam sub-structuring system, were carried out to investigate whether the slabs could be assumed with in-plane rigidity.

The building was assumed fixed at the base and the beam-to-column connections were assumed rigid and full-strength (moment resisting). The finite element computer program MidasGen 2017 [16], was used for the structural analysis. Beam and columns have been modeled as steel frame elements with fibers, with a behaviour represented by the Menegotto-Pinto constitutive law [17], assuming  $F_y = 235\text{ N/mm}^2$ ,  $E = 210000\text{ N/mm}^2$  and  $b = 0.02$ . The effects of masonry infills have also been modeled as they may significantly influence the dynamic and earthquake response of the structures. The numerical modelling of infilled frames is a complex issue because these structures exhibit a highly non-linear inelastic behaviour resulting from the interaction of the masonry infill panel and the surrounding frame (e.g. [18, 19]). In this case, an equivalent strut macro-model has been utilized to model the infill presence. Such macro-models exhibit obvious advantages in terms of computational simplicity and efficiency. Their formulation is based on a physically reasonable representation of the structural behaviour of the infilled frame. The equivalent width  $b_w$  of the strut is determined according to the relevant formulation in [20]. In case that the infill panels have openings, the width  $b_w$  of the equivalent strut is reduced by the R-factor in accordance with [21]. The presence of partial infills has been accounted for connecting the equivalent strut to a node located within the column length. This allowed to simulate the local damage conditions in the columns showed during the earthquake, as also discussed in Section 5.

The nonlinear response of infill panels has been simulated with the tri-linear model by [22]. The model has been implemented in MidasGen with the Takeda treat-linear model.

#### **5. OBSERVED STRUCTURAL DAMAGE FOR THE SAMPLE BUILDING**

The sample building experienced significant non-structural damage and limited structural damage during the 2016 Central Italy earthquake sequence, without collapsing. Nevertheless, damage accumulation was observed during the major seismic events that affected the location of the steel building, particularly after the

24<sup>th</sup> August and 30<sup>th</sup> October 2016 earthquakes. Figure 1 shows the response of the sample structure in the aftermath of the seismic sequence.



Figure 1. – Seismic response of the sample building: before the earthquakes (left), after the 24th August event (middle) and after the 30<sup>th</sup> October 2016 (right).

In the aftermath of the 24<sup>th</sup> August event, it was observed that the non-structural components, especially the masonry infill panels, and the architectural finishes, e.g. the plaster, were significantly cracked. Some damage was also detected in the columns, particularly at the beam-to-column connection.

After the 30<sup>th</sup> October 2016, the steel frame experienced large inelastic demand and the structural and non-structural damage became widespread. The columns suffered localized damage due to the presence of infill panels which generated high concentrated stresses at the beam-to-column connections. Out-of-plane failure of the masonry infills were detected along the perimeter of the frame. Some joists at the openings collapsed. The steel building has experienced significant lateral drifts but the residual strength of the structure was sufficient to carry the gravity loads and prevent the global collapse.

## 4. ANALYSIS RESULTS

### 4.1. MODAL ANALYSIS

The dynamic behaviour of the building has been initially investigated by means of modal analysis, that revealed the great influence of the infill panels in the dynamic response of the structure. Figure 2 shows the 1<sup>st</sup> and 2<sup>nd</sup> vibration modes for the case of bare and infilled buildings, respectively. In first case, the first mode is mainly translational along the X-direction with a period of 1.88 sec, whereas the second mode is also translational in the Y-direction with a period of 0.94 sec. The behaviour changes significantly when infills are accounted for. For the steel building with infills, the first mode is still translational but in the transversal direction (Y-direction) and the corresponding period of vibration is 0.56 sec, whereas the second mode is in the X-direction with a period of 0.28 sec. Figure 2 also provides the participating masses relative to the first and second mode of vibration of the bare and infilled framed buildings. It is observed that the participating masses associated to the lower modes of vibrations tend to increase when infills are considered. Such response corresponds to an irregular global dynamic behaviour of the actual sample structures, i.e. multi-storey steel building with masonry infills along the perimeter frames.

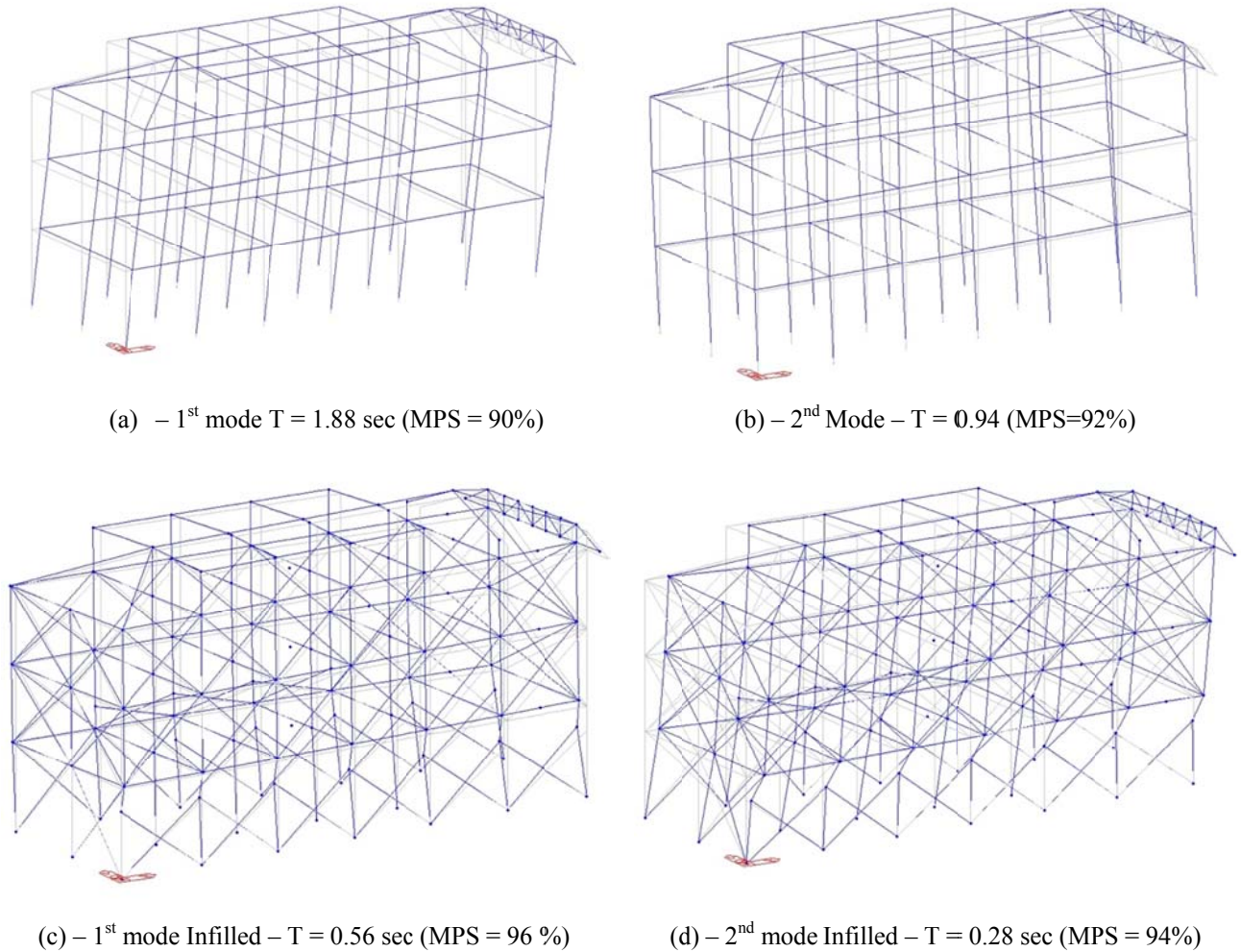


Figure 2. - Vibrational modes in the bare (a, b) and infilled (c, d) building.

The above discussion indicates that the seismic vulnerability of the case study building changes dramatically in presence of infill panels. The observed variations are two-fold. The fundamental periods of the infilled system tend to change with respect to the bare frame counterpart. Additionally, there is also a change in the most vulnerable direction of the structure, i.e. the transversal direction (Y-direction), which coincides with the direction along which the building experienced the most significant damage pattern and drift.

#### 4.2. NONLINEAR STATIC ANALYSIS

The presence of large residual damage in the surveyed structure indicates the high level of seismic action to which the building was subjected during the seismic events of the 2016-2017 Central Italian earthquake. Consequently, a nonlinear analysis of the building has been conducted by using the model described in Section 3, in which both the non-linearities of the steel elements and infill panels were accounted for. As a first level of investigation, nonlinear static (pushover) analysis was herein conducted, to assess the evolution of the damage in the elements for increasing level of the action and to compare the seismic demand with the capacity of the main elements (beam and columns) according to the provisions implemented in the Eurocode 8 - Part 3 [23].

The capacity (pushover) curves of the structure in the X and Y directions are shown in Figure 3. Two lateral force distributions were considered, namely, a mass-proportional and a modal force distribution. Given the fundamental importance of the infill panels in the non-linear seismic response of the building, only the results of infilled frame have been here plotted and commented. It is observed that different force

distributions along the height of the building generate similar response. For this reason, in the following only the modal distribution of forces will be considered.

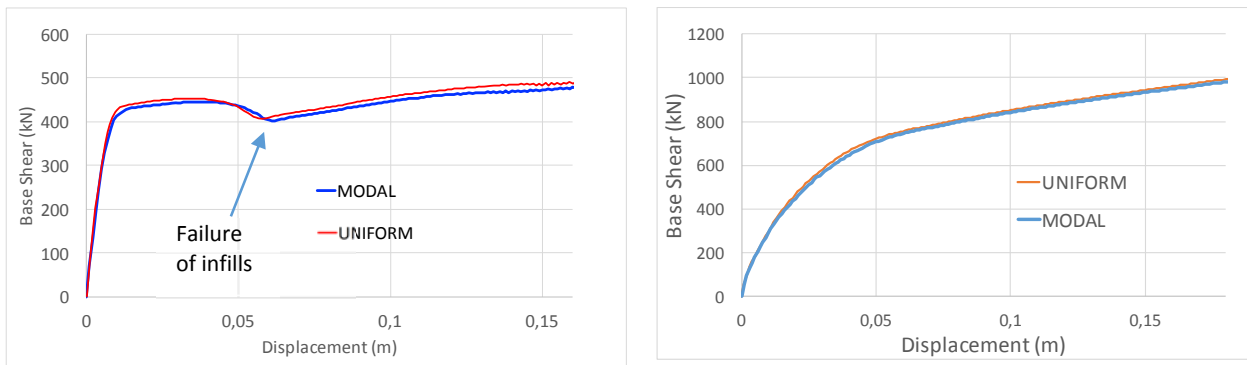


Figure 3. – Capacity curves for the infilled frame: X-direction (*left*) and Y-direction (*right*).

The effects of the infill panels on the seismic behaviour of the buildings is evident, especially in the X-direction, where the infill panels were actually subjected to the highest damage level. While base-shear and displacement increase initially in a linear manner, infill panels damage initiates approximately at a displacement of 1cm until failure that occurred at a control point displacement of 4cm. As anticipated, a significant drop in the lateral resistance is also observed. Upon exhaustion of the infill panel resistance, the yielding of the steel elements takes place leading to a force increase due to the hardening effect. The absence of damage in the infill panels in the Y-direction, observed during the in-situ inspections, is verified in Figure 4, where the contribution of the infills is confined in the elastic range and the force increases monotonically. Figure 4 further shows the distribution of the plastic hinge for life safety (LSL) and collapse (CLS) limit states, respectively. It is interesting to note that at CLS the damage is confined in the columns at first floor that were subjected to a significant damage (i.e. important yielding conditions). This is in agreement with the damage observed during the in-situ inspections (*see* also Figure 5).

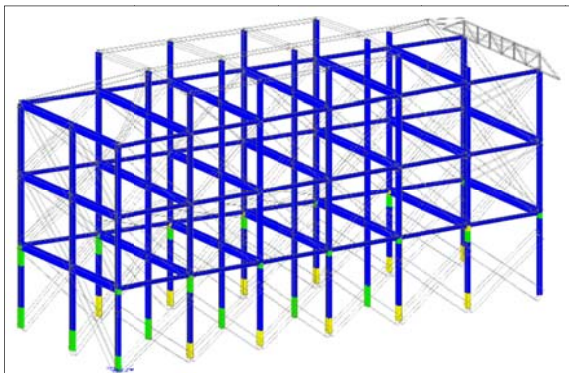


Figure 4. - Distribution of the plastic hinges at the Collapse Limit State



Figure 5. – Damage in the columns of the first floor of the building

In order to calculate the seismic demand of the structure corresponding to the above-mentioned limit states, the N2 method has been herein adopted [24]. The corresponding elastic response spectra are illustrated in Figure 6. The demand in terms of base shear and displacement is reported in Figure 7 for the different limit states. It can be noticed that the damageability limit state (DLS) is, as expected, located close to the yielding of the building, whereas CLS is located in proximity of the infill panel failure (Figure 8). This is again fully compatible with the in-situ observations of severe infill damage.

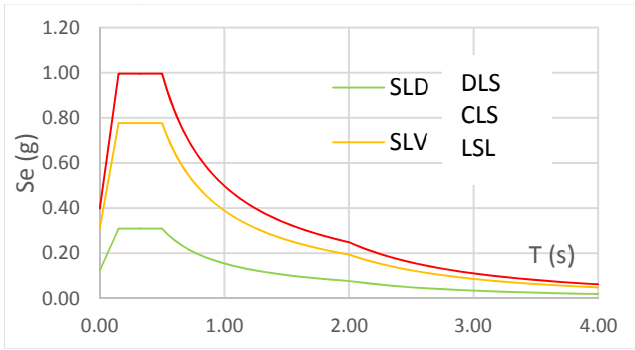


Figure 6. - Elastic spectra for different limit state according to Eurocode 8.

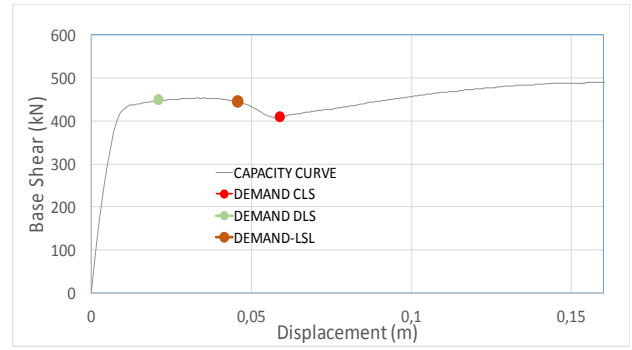


Figure 7. - Seismic Demand for DLS, LSL and CLS.

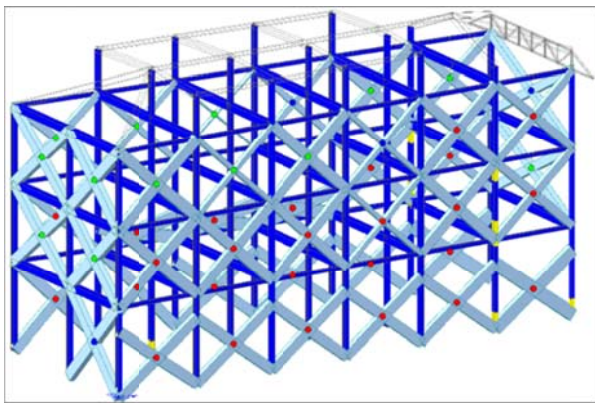


Figure 8. - Damage distribution in the infills (red dots = failure conditions)

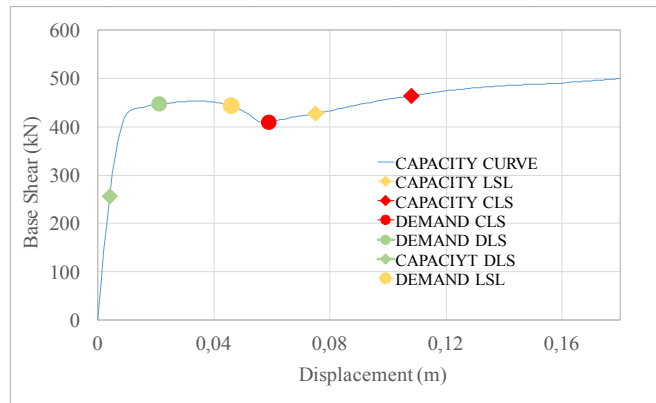


Figure 9. - Comparison between demand and capacity at different limit states

To evaluate the reliability of the Eurocode 8- Part 3 [23] in the assessment of existing steel structures, the seismic capacity at the above-mentioned limit states has been calculated and compared with the demand of Figure 9. In this respect, Eurocode 8- Part 3 [23] prescribes that both ductile and fragile limit states should be verified. Concerning ductile limit states, Eurocode imposes, for different limit states and class of cross section, the chord-rotation thresholds summarised in Table 2. The capacity is then quantified in relation to the yielding chord rotation, which can be calculated as suggested in [25]. In particular, eq. (1) can be used for beams and eq. (2) for columns, where  $M$  is the plastic moment,  $L_b$  and  $L_c$  are the lengths of the beams and columns, respectively,  $I$  is the moment of inertia,  $E$  is the elastic modulus,  $N_{ed}$  and  $N_{p,Rd}$  are respectively the demand and the ultimate value in terms of axial force.

$$\theta_y = \frac{M_{Pb,Rd} \times L_b}{6IE_b} \quad (1)$$

$$\theta_y = \frac{M_{Pc,Rd} \times L_c}{6IE_c} \left(1 - \frac{N_{ed}}{N_{p,Rd}}\right) \quad (2)$$

Table 2. - Limit of chord-rotations for different classes of cross section

| Class of cross section | Limit State     |                |                |
|------------------------|-----------------|----------------|----------------|
|                        | DLS             | LSL            | CLS            |
| 1                      | 1,0 $\theta_v$  | 6,0 $\theta_v$ | 8,0 $\theta_v$ |
| 2                      | 0,25 $\theta_v$ | 2,0 $\theta_v$ | 3,0 $\theta_v$ |

Given that all members of the structure are deemed as Class 1, the values of the first row in Table 2 have been used. The fragile mechanisms are instead checked in terms of shear strength. Given the particular type of mechanism, in what follows, only the ductile mechanisms will be commented. Figure 9 shows the comparison between capacity and demand. It can be noticed that while LSL and CLS limit states are fully

fulfilled, the serviceability condition is by no means satisfied. More precisely, Eurocode appears to be particularly conservative. DLS should refer to a damage condition for which the nonstructural elements would be already damaged without important damages in the structural members. In the case study, the capacity refers to a condition of both structural and non-structural elements undamaged.

#### 4.2. NONLINEAR BEHAVIOUR OF THE BUILDING UNDER 24 AUGUST 2016 EARTHQUAKE

The dynamic behaviour of the building has also been investigated considering the East-West component of the ground motion recorded at the accelerometric Station of Amatrice, during the event M/S1, applied along the longitudinal direction (X). As described previously, the maximum PGA is equal to 0.85g, with a resonance peak at 0.25 sec, against a fundamental period of building of 0.56 sec. Therefore, a limited amplification is expected, especially in presence of nonlinearities that cause increasing of the vibration periods.

Figure 10 shows the time-history of the base shear (Figure 10b) and the displacement at the top of the building (Figure 10c), along with the cyclic response of a masonry infill present along the perimeter of the existing steel frame structure (Figure 10d). The earthquake strong motion used in the analysis is provided in Figure 10a.

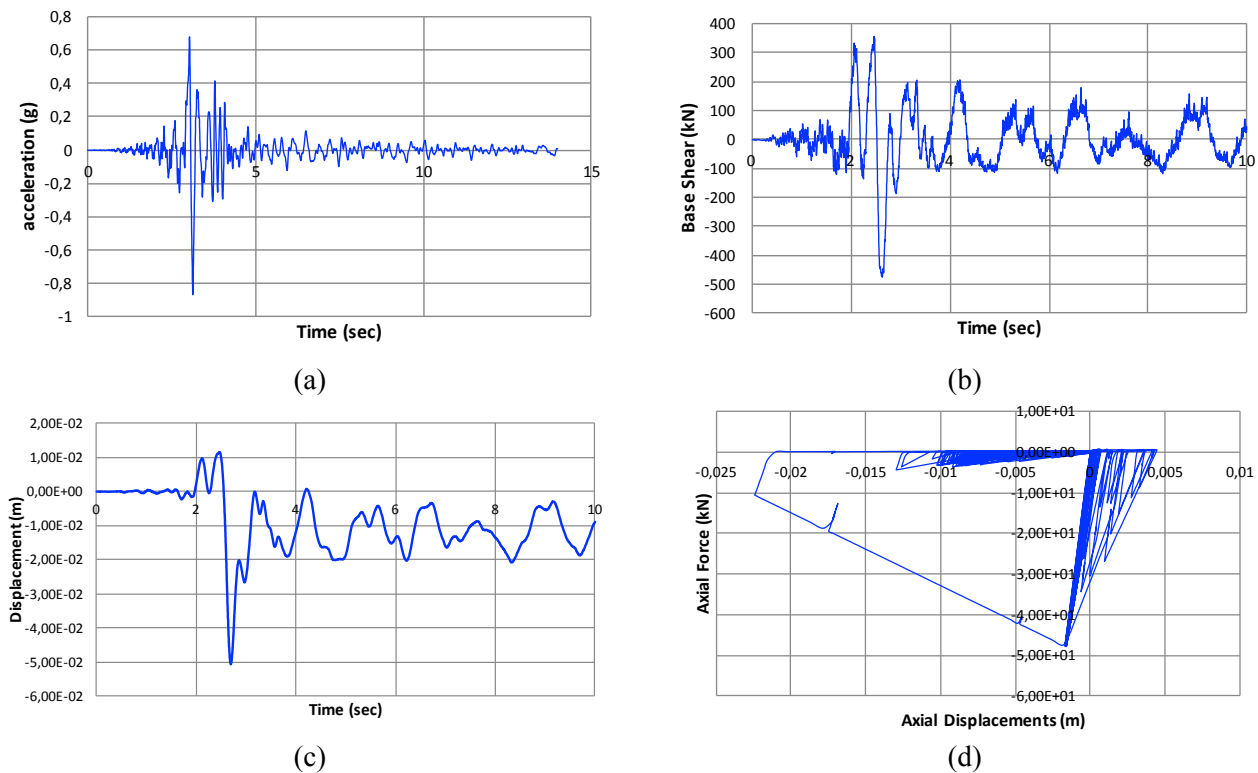


Figure 10 (a) East-West record - Amatrice 24.08.2016, (b) Base Shear, (c) Top displacement, (d) Axial Force-Displacement of an infill panel.

The response of the building evaluated with the time-history analysis matches the results of the nonlinear static pushover analysis, presented in the previous section. For example, the maximum base shear, evaluated using either static (Figure 7) or dynamic analysis (Figure 10b), is about 470 kN. This is mainly due to a similar frequency content and amplification of the response spectra. The damage pattern determined with the time-history analysis is also similar to the predictions obtained with the pushover analysis. A significant contribution of the infill panels has been observed, as also displayed in Figure 12, where an example of cyclic response of an infill panel is provided. The complete damage pattern of the infill panels is shown in



Figure 11, where the most damaged infills are clearly located in the first and second floor of the building. This result fits closely with the observed response of the real building, as shown in Figure 5. The damage in the steel elements is also limited at first and second floor, similarly to the real damage pattern observed on site (*see* also Figure 5 and Figure 11).

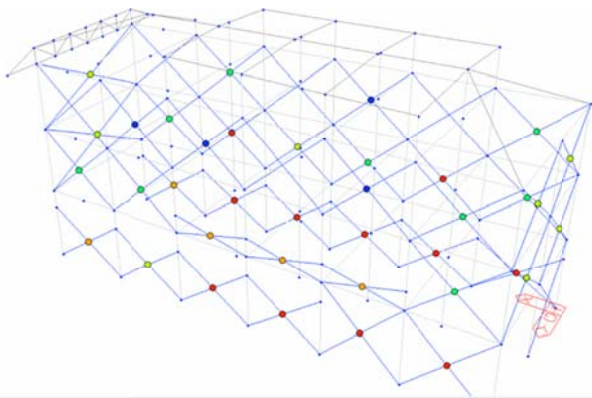


Fig. 11 – Damage pattern in the infill panels recorded in time history analysis

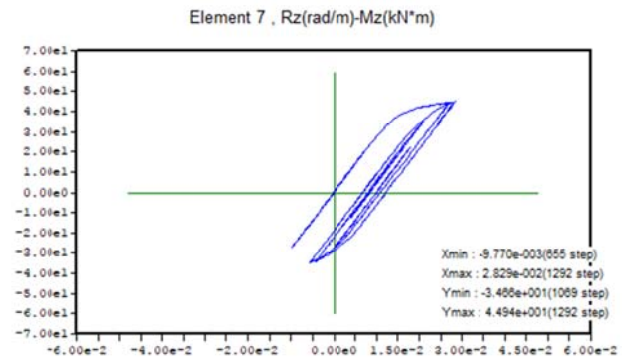


Fig. 12 – Moment-Curvature of a column at first floor

## CONCLUSIONS

The present paper presents the preliminary numerical assessment of the structural performance assessment of a case steel MRF building located in Amatrice, Central Italy, which experienced extensive structural and non-structural damage during the recent swarm of events but did not collapse.

Refined numerical models of the existing steel building were implemented considering the effects of the perimeter masonry infills. The primary aim was to capture the actual damage pattern surveyed in the aftermath of the 2016 Central Italy earthquakes for the case study building.

The results of the modal response of the structure have emphasized the significant effects of the masonry infills on the global dynamic behaviour of the structure. It was found, for example, that the fundamental period of vibration of the steel frame with infills is nearly 1/3 of the bare steel structure, 0.56 seconds versus 1.88 seconds. Thus, it is of paramount importance, when estimating the seismic demand on steel structures, to account for the presence of infills which tends to augment the lateral stiffness of the structural system and, in turn, to increase the actual earthquake loadings.

The seismic performance of the case study steel structure has also been assessed through advanced, comprehensive and efficient static and dynamic nonlinear analyses. It was found that the latter analyses may both provide a realistic damage distribution when the infills are included in the structural models and can thus be utilized to perform reliable risk assessment of the existing steel structures. The provisions of the Eurocode 8-Part 3 for existing building structures were included in the non-linear static structural assessment. The latter rules tend to provide a conservative estimate of the global response of the case study structures. Further numerical analyses are required to corroborate the reliability of the existing provisions for the assessment of existing steel structures.

## REFERENCES

- 1.) Elghazouli, A.Y. (2010). Assessment of European seismic design procedures for steel frames structures, *Bulletin of Earthquake Engineering*, 8(1), 65-89.
- 2.) Romao, X., Delgado, R., Guedes, J and Costa, A. (2010). A comparative application of different EC8-3 procedures for the seismic safety assessment of existing structures, *Bulletin of Earthquake Engineering*, 8, 91-118.
- 3.) Braconi, A., Caprili, A., Degee, H., Guendel, M., Hjaij, M., Hoffmeister, B. and Karamanos, S.A., Rinaldi, V. and Salvatore, W. (2015). Efficiency of Eurocode 8 design rules for steel and steel-concrete composite structures, *Journal of Constructional Steel Research*, 112, 108-129.
- 4.) Araujo, M. and Castro, J.M. (2017). A critical review of European and American Provisions for the Seismic Assessment of Existing Steel Moment-Resisting Frame Buildings, *Journal of Earthquake Engineering*, 1-29.

- 5.) European Committee for Standardization (CEN) (2005). Eurocode 8. Design of structures for earthquake resistance – Part 3: Assessment and retrofitting of buildings, Brussels, Belgium.
- 6.) American Society of Civil Engineers (ASCE) (2014). Seismic evaluation and retrofit of existing buildings. ASCE/SEI 41-13, Reston, Virginia, USA.
- 7.) Elnashai, A.S. and Di Sarno, L. (2015). Fundamentals of Earthquake Engineering: From the Source to Fragility, John Wiley & Sons, Chichester, UK, ISBN 976-0-470-02483-6.
- 8.) Landolfo, R., Mazzolani, F.M. and Zandonini, R. (2015). Steel and Steel-Concrete Composite Structures. In The state of Earthquake Engineering Research in Italy: the ReLUIS-DPC 2010-2013 Project, G. Manfredi, M. Dolce (eds), 99-141, doi: 10.14599/r101303, Doppiavoce, Napoli, Italy.
- 9.) Freddi F., Tubaldi E., Zona A., Dall'Asta A. (2017) Seismic performance of structural systems equipped with buckling-restrained braces. XXVI Giornate Italiane della Costruzione in Acciaio, CTA Collegio dei Tecnici dell'Acciaio, Venice, Italy, 28-30 September.
- 10.) Nassirpour, A., Song, B. and D'Ayala, D. (2017a). IDA & Cloud Method for Fragility Assessment of Bare & Infilled Steel Frame Structures. 16th World Conference on Earthquake Engineering, Santiago, Chile, 9-13 January.
- 11.) Nassirpour, A and D'Ayala, D. (2017b). Seismic loss estimation of mid-rise masonry infilled steel frame structures through incremental dynamic analysis, International Journal of Forensic Engineering, 3(3): 255.
- 12.) GEER. (2016). Engineering Reconnaissance of the 24 August 2016 Central Italy Earthquake. Version 2. Report No. GEER-050B. Version 2 (11), doi:10.18118/G61S3Z.
- 13.) Gruppo di Lavoro INGV sul terremoto in centro Italia (2016). Summary report on the October 30, 2016 earthquake in central Italy Mw 6.5, doi: 10.5281/zenodo.166238.
- 14.) Ministero per le Infrastrutture e i Trasporti (2008). Norme Tecniche per le Costruzioni, Roma, Italy (*in Italian*).
- 15.) Ministero per i Lavori Pubblici (2008). Decreto Ministeriale 16 Gennaio 1996 – Norme Tecniche per le Costruzioni in Zone Sismiche, Roma, Italy (*in Italian*).
- 16.) Midas Engineering Software (2017). Integrated Solution System for Building and General Structures.
- 17.) Menegotto, M. and Pinto, P. E. (1973). Method of analysis for cyclically loaded reinforced concrete plane frames including changes in geometry and non-elastic behavior of elements under combined normal force and bending. Proceedings of the IABSE Symposium of Resistance and Ultimate Deformability of Structures Acted on by Well-Defined Repeated Loads, International Association of Bridge and Structural Engineering, Lisbon, Portugal, 13, 15-22.
- 18.) Crisafulli, F.J., Carr, A.J. and Park, R. (2000). Analytical modelling of infilled frame structures. A general overview. Bulletin of The New Zealand Society for Earthquake Engineering. 33(1), 30-47.
- 19.) Elnashai, A.S. and Di Sarno, L. (2008). Fundamentals of Earthquake Engineering, Wiley and Sons, UK.
- 20.) Klingner, R.E. and Bertero, V.V. (1976). Infilled Frames in Earthquake-Resistant Construction, Report no.EERC 76-32, University of California, Berkeley, USA.
- 21.) Al-Chaar, G. (2002). Evaluating Strength and Stiffness of Unreinforced Masonry Infill Structures. U.S. Army Corps of Engineers, Construction Engineering Research Laboratories, Report no. ERDC/CERL TR-02-01, USA
- 22.) Fardis, M.N. and Panagiotakos T.B. (1997). Seismic design and response of bare and infilled reinforced concrete buildings. Part II: Infilled structures. Journal of Earthquake Engineering, 1(3):475-503.
- 23.) Comite Europeen de Normalisation (CEN) (2006). Eurocode 8 — Design of structures for earthquake resistance - Part 3: Assessment and retrofitting of buildings, Brussels.
- 24.) Fajfar, P. and Gaspersic, P. (1996). The N2 Method for the Seismic Damage Analysis of RC Buildings. Earthquake Engineering and Structural Dynamics, 25(1), 31-46.
- 25.) Araujo, M. and Castro, J.M. (2017). A critical review of European and American Provisions for the Seismic Assessment of Existing Steel Moment-Resisting Frame Buildings, Journal of Earthquake Engineering, 1-29.